Research Article

Electrochemical synthesis of hydrogen peroxide with a three-dimensional rotating cylinder electrode

Omar González Pérez and José M. Bisang*

Abstract

BACKGROUND: This work analyzes the synthesis of H_2O_2 from dilute NaOH solutions under 0.1 MPa O_2 using a batch reactor with a three-dimensional rotating cylinder electrode. The centrifugal force produces a radial co-current flow of the gas and liquid phases. Thus, good mass transfer conditions are achieved and the O_2 reduced to H_2O_2 is easily replenished in the liquid phase.

RESULTS: Experiments with a glassy carbon rotating disc electrode identified $0.5\ mol\ L^{-1}$ NaOH at 30°C as suitable operating conditions. Galvanostatic experiments with three-dimensional rotating electrodes concluded that the best performance was obtained for a reticulated vitreous carbon structure of 100 ppi, at $40\ mA\ cm^{-2}$ of macrokinetic current density and 1000 rpm rotation speed. Long-term experiments showed 79% current efficiency and $8.2\ kWh\ kg^{-1}$ specific energy consumption until 6 h of electrolysis, with $8.4\ g\ L^{-1}$ H_2O_2 concentration. However, the current efficiency decreases for longer electrolysis times and consequently the specific energy consumption is increased. Thus after 10 h electrolysis the concentrations were H_2O_2 $10.4\ g\ L^{-1}$ and NaOH $1.41\ mol\ L^{-1}$.

CONCLUSION: A reactor having a three-dimensional rotating cylinder electrode with co-current oxygen and liquid flows inside the structure showed promising performance for H_2O_2 production.
ⓒ 2013 Society of Chemical Industry

Keywords: hydrogen peroxide; electrochemical reactor; three-dimensional electrode; oxygen reduction

NOTATION

A_s	surface area per unit electrode volume (m^{-1})
C	concentration ($mol\ m^{-3}$ or $g\ L^{-1}$)
D	diffusion coefficient ($m^2\ s^{-1}$)
E_s	specific energy consumption ($kWh\ kg^{-1}$)
E_{SCE}	electrode potential referred to saturated calomel electrode (V)
F	Faraday constant ($C\ mol^{-1}$)
i_b	macrokinetic current density ($mA\ cm^{-2}$)
I	total current (A)
j	current density ($mA\ cm^{-2}$ or $A\ m^{-2}$)
j_k	current density under charge transfer control ($A\ m^{-2}$)
j_L	limiting current density $= \nu_e F k_m C$ ($A\ m^{-2}$)
k_m	mass-transfer coefficient ($m\ s^{-1}$)
L	electrode length (m)
P	pressure (Pa)
q	volumetric flow rate ($m^3\ s^{-1}$)
Q	charge (A h)
r_i	inner radius of the three-dimensional electrode (m)
r_o	outer radius of the three-dimensional electrode (m)
t	time of the experiment (h)
T	temperature (°C)
u	liquid flow velocity ($m\ s^{-1}$)

Greek characters

β	current efficiency (%)
ΔP	pressure drop across the three-dimensional electrode (Pa)
$\Delta\eta$	range of overpotential (V)
ϵ	void fraction
ν	kinematic viscosity ($m^2\ s^{-1}$)
ν_e	charge number of the electrode reaction
ρ_s	effective electrolyte resistivity ($\Omega\ m$)
ρ	electrolyte density ($kg\ m^{-3}$)
ω	rotation speed (rpm or s^{-1})

INTRODUCTION

The main uses of hydrogen peroxide include bleaching of wood pulp and textiles, preparation of other peroxide compounds, and serving as a non-polluting oxidizing agent.[1] Hydrogen peroxide

* Correspondence to: J.M. Bisang, Programa de Electroquímica Aplicada e Ingeniería Electroquímica (PRELINE), Facultad de Ingeniería Química, Universidad Nacional del Litoral, Santiago del Estero 2829, S3000AOM Santa Fe, Argentina. Email: jbisang@fiq.unl.edu.ar

Programa de Electroquímica Aplicada e Ingeniería Electroquímica (PRELINE), Facultad de Ingeniería Química, Universidad Nacional del Litoral, Santiago del Estero 2829, S3000AOM Santa Fe, Argentina

is now predominantly manufactured by strategically located anthraquinone autoxidation processes, and less extensively by anodic electrolytic procedures.[2] Alternatively, Berl[3] proposed the technical preparation of hydrogen peroxide from the electrochemical reduction of oxygen at a carbon cathode and reviews of this procedure were given by Foller and Bombard[4] and Oloman.[5] Three-dimensional carbon structures were examined[6−8] as cathodes because their high specific surface area increases the reactor space-time yields. Moreover, to counteract the low solubility of oxygen in aqueous electrolytes trickle bed electrodes are preferred.[9−15] Therefore, a controlled flow trickle bed reactor was developed using a porous cathode composed of a bed of graphite chips coated with PTFE and carbon black.[16] A second strategy for the cathodic manufacture of hydrogen peroxide is the use of oxygen gas-diffusion electrodes.[17,18] High hydrogen peroxide concentration with low specific energy consumption was reported in concentrated alkaline solutions.[4] However, to satisfy different industrial requirements it is important to examine its production in a variety of electrolytes, such as dilute alkaline solutions, in order to increase the oxygen solubility. Thus, in spite of the long history of the synthesis of hydrogen peroxide via the cathodic reduction of oxygen, attempts to improve its practical application remain the centre of attention.

The goal of the present study was to analyze a different arrangement of the electrochemical reactor. Thus, the behaviour of a rotating cylinder electrode made of three-dimensional carbon structures was examined, where the liquid and gas flows take place in radial directions by the rotation of the electrode.

FUNDAMENTAL STUDIES WITH A ROTATING DISC ELECTRODE

Experimental details

A rotating disc electrode was used to obtain the cathodic polarization curves, because this electrochemical system presents well-defined hydrodynamic conditions and the mass transport characteristics are well known.

The working electrode was a glassy carbon disc, 3 mm in diameter embedded in a Teflon cylinder of 10 mm diameter. A platinum wire counter electrode, 1 mm diameter and 100 mm long, was used. A saturated calomel electrode was used as reference and the potentials are referred to this electrode.

The surface of the working electrode was polished to a bright mirror finish with slurry of 0.3 μm alumina powder and copiously washed with distilled water. NaOH solutions ranging from 0.1 to 4 mol L^{-1} were used as the electrolyte. The temperature and the rotation speed were changed in the experiments performed under a slow potentiodynamic sweep of 2 mV s^{-1} to obtain steady-state polarization curves. Under ambient conditions the oxygen volumetric flow rate was 9.36×10^{-6} m^3 s^{-1}, and before the experiments oxygen was bubbled into the solution for 1 h to ensure saturation of the electrolyte. The polarization curves were recorded under an oxygen atmosphere.

The desired cathodic reaction was:

$$O_2 + H_2O + 2\,e^- \;\rightarrow\; HO_2^- + OH^- \tag{1}$$

However, the following reactions can also take place at the cathode:
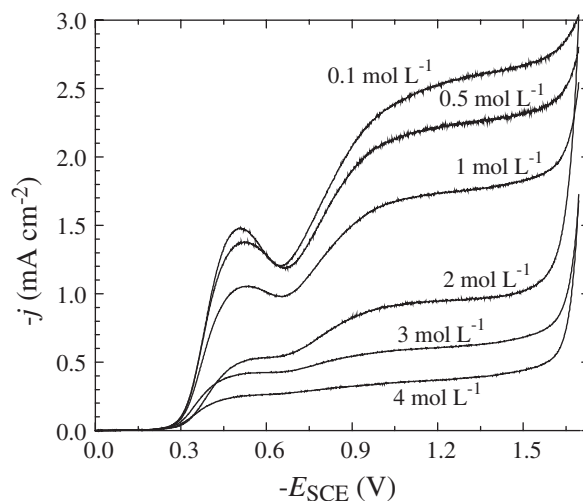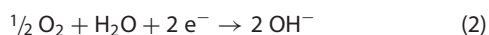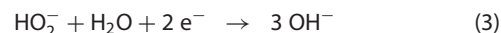
$$^1\!/_2\,O_2 + H_2O + 2\,e^- \rightarrow 2\,OH^- \tag{2}$$

Figure 1. Current density as a function of the electrode potential for different NaOH concentrations. $T = 30°C$; $P = 0.1$ MPa; $\omega = 1500$ rpm; potential sweep rate: 2 mV s^{-1}.
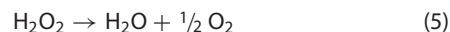
and

$$HO_2^- + H_2O + 2\,e^- \;\rightarrow\; 3\,OH^- \tag{3}$$

The anodic reaction was oxygen evolution:

$$2\,OH^- \rightarrow {}^1\!/_2\,O_2 + H_2O + 2\,e^- \tag{4}$$

and the catalytic decomposition of hydrogen peroxide occurs in the bulk solution according to:

$$H_2O_2 \rightarrow H_2O + {}^1\!/_2\,O_2 \tag{5}$$

Results and discussion

Figure 1 shows cathodic polarization curves as a function of the NaOH concentration where two reduction waves are observed in all cases. Similar results were reported by previous authors showing a common behaviour for two consecutive electrode reactions.[19−29] Thus, it was assumed that the oxygen reduction takes place in two steps giving in the first process perhydroxyl ions, reaction 1, and hydroxyl ions in the second one, reaction 2. However, it was also found that the relative heights of the two reduction waves for O$_2$ are very dependent on the pre-treatment of the glassy carbon surface. Hence, it would appear that the two waves result from the reduction of O$_2$ at different types of sites on the surface and the production of perhydroxyl ions can occur in both regions of potential.[30−37] Likewise, the limiting current increases when the NaOH concentration decreases because the oxygen solubility is increased. However, the use of a dilute supporting electrolyte presents the disadvantage of low conductivity, which increases the cell voltage. Thus, 0.5 mol L^{-1} NaOH is an attractive supporting electrolyte due to the resulting high values of limiting current densities and an acceptable conductivity. Limiting currents are well defined at NaOH concentrations higher than 2 mol L^{-1}, but at lower concentrations the first wave presents a peak, which was also previously reported.[17,23,30,32,38−40] The decay in the current density at more negative potentials of the porous electrodes was attributed to flooding of the carbon pores because the hydrogen peroxide oxidizes its surface thus becoming more hydrophilic.[17] Taylor and Humffray[30] proposed that the unexpected minimum of current
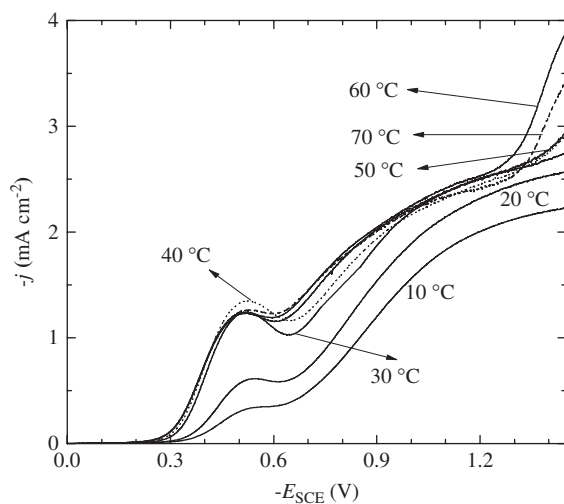
Figure 2. Current density as a function of the electrode potential for different temperatures. [NaOH] = 0.1 mol L^{-1}; P = 0.1 MPa; ω = 1500 rpm; potential sweep rate: 2 mV s^{-1}.
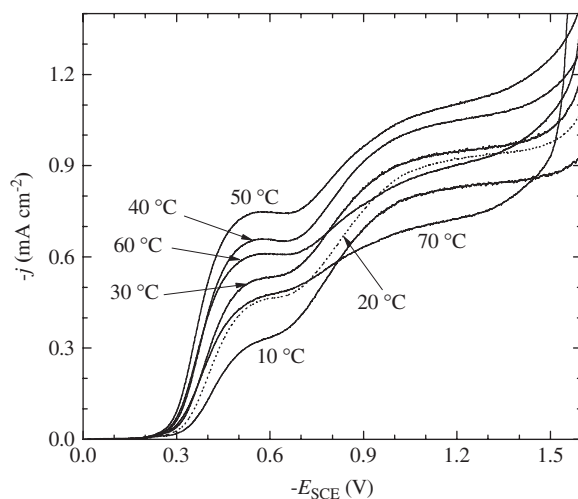

Figure 4. Current density as a function of the electrode potential for different rotation speeds. [NaOH] = 0.1 mol L^{-1}; T = 30°C; P = 0.1 MPa. Inset: Koutecký–Levich plot. Potential sweep rate: 2 mV s^{-1}.

Figure 3. Current density as a function of the electrode potential for different temperatures. [NaOH] = 2 mol L^{-1}; P = 0.1 MPa; ω = 1500 rpm; potential sweep rate: 2 mV s^{-1}.

Figure 5. Current density as a function of the electrode potential for different rotation speeds. [NaOH] = 2 mol L^{-1}; T = 30°C; P = 0.1 MPa. Inset: Koutecký–Levich plot. Potential sweep rate: 2 mV s^{-1}.

for an activated electron transfer process is due to a decrease in the number of electrocatalytic active surface sites for oxygen reduction. Tammeveski et al.[32] reported good correlation of experimental results with a theoretical model assuming a potential dependence of the surface concentration of the active sites.

Figures 2 and 3 show the current as a function of the cathodic potential at different temperatures for 0.1 and 2 mol L^{-1} NaOH, respectively. The increase of temperature has two opposite effects. The first effect is to enhance the mass-transfer and the second is to decrease the oxygen solubility. So the appropriate operating temperature is a compromise between them and thus best performance is at 50°C for a 2 mol L^{-1} NaOH concentration and at 30°C when the concentration is 0.1 mol L^{-1}, but in this last case a small difference is detected with the limiting current at higher temperatures. According to Figs 1–3, the most suitable operating conditions for hydrogen peroxide production are a concentration of 0.5 mol L^{-1} NaOH at 30°C.
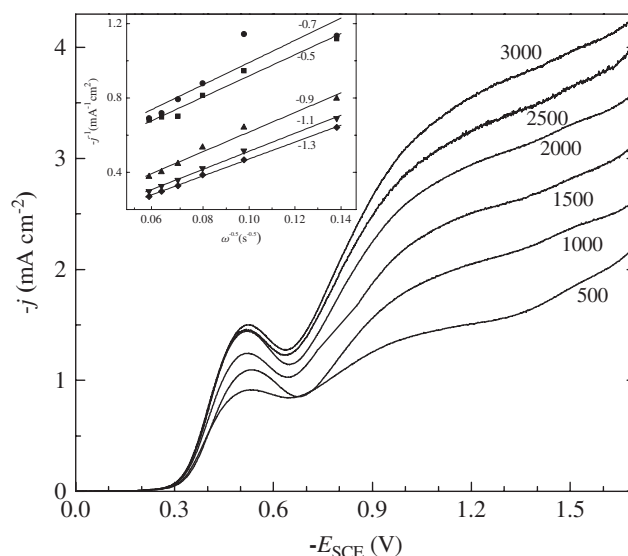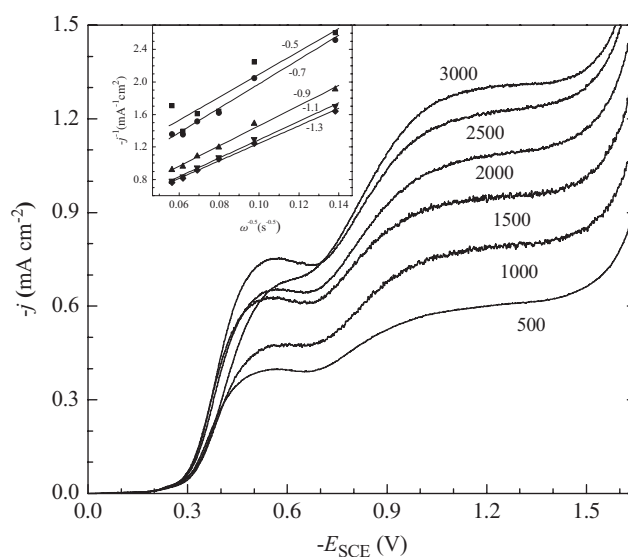
Figures 4 and 5 show the polarization curves for oxygen reduction at different rotation speeds for a supporting electrolyte of 0.1 and 2 mol L^{-1} NaOH, respectively. The inset in each figure represents the Koutecký–Levich plot:[41]

$$\frac{1}{j} = \frac{1}{j_k} + \frac{1}{0.62\nu_e F D^{2/3} \nu^{-1/6} \omega^{1/2} C} \quad (6)$$

where all the lines are parallel and the intercept is a reciprocal function of the heterogeneous rate constant for the electron transfer process. The oxygen diffusion coefficient, obtained from the slope of the lines assuming $\nu_e = 2$, is 1.66×10^{-9} m^2 s^{-1} for 0.1 mol L^{-1} and 1.45×10^{-9} m^2 s^{-1} for 2 mol L^{-1} NaOH, which agree with the literature values.[42] Other parameters used in these calculations are reported in Table 1.

Table 1. Physicochemical properties of the supporting electrolyte; $T = 30°C$

[NaOH] (mol L^{-1})	$\nu \times 10^6$ (m^2 s^{-1})	C_{Oxygen} ($P = 0.1$ MPa) (mol m^{-3})
0.1	0.797	1.130
2	1.140	0.525

Table 2. Geometric parameters of the carbon structures

	A_s (m^{-1})	ϵ
RVC 10 ppi	1300	0.97
RVC 45 ppi	2710	0.97
RVC 100 ppi	6700	0.97
GF-S6	21818	0.94

EXPERIMENTS WITH CYLINDRICAL BATCH REACTORS

Experimental details

The experiments were performed in a batch reactor, 95 mm internal diameter and 140 mm high. The reactor was thermostated using a heating jacket. The complete experimental arrangement is depicted schematically in Fig. 6. The working electrode was formed by a graphite cylinder, Carbone Lorraine grade 6503 E, 22 mm diameter and 44 mm long, which supports the three-dimensional electrodes made of either reticulated vitreous carbon or graphite felt, both supplied by The Electrosynthesis Co., Inc. In the first case, three ring-shaped discs, 22 mm internal diameter, 42 mm external diameter and 12.7 mm high were placed on the cylindrical graphite support to form the three-dimensional electrode. In the second case, a sheet of graphite felt, 3 mm thick, was wound around the cylindrical graphite support and maintained in position by a helical plastic outer support. In both cases the three-dimensional material was fixed to the support by graphite paint, which enhances the electrode conductivity. In the experiments GF-S6 graphite felt and three grades of reticulated vitreous carbon, RVC, i.e. 10, 45 and 100 ppi were used. The bed depth of the three-dimensional structures in the direction of the current flow, $r_o - r_i = 10$ mm for RVC and 3 mm for GF-S6 was chosen taking into account the following expression:[43]

$$\Delta\eta - \frac{j_L A_s \rho_s r_i^2}{2}\left[\frac{(r_o/r_i)^2 - 1}{2} - \ln\frac{r_o}{r_i}\right] = 0 \qquad (7)$$

assuming typical values for the other geometric parameters of the three-dimensional electrodes given in Table 2 and 0.3 V for the potential range to ensure the whole bed was working under limiting current conditions. The limiting current density was calculated with a mass transfer coefficient according to Nahlé et al.[44]

The upper end of the cylindrical graphite support was attached to the motor shaft. Oxygen was fed at 0.1 MPa into a chamber inside the graphite cylinder, via a port located at its lower end, and flowed through the three-dimensional electrode via three radial channels symmetrically drilled in the support. Thus, the rotation of the electrode enables a co-current radial flow of the liquid and gas phases, giving appropriate intermixing between them. Two advantages can be recognized for this arrangement: (i) the reactant
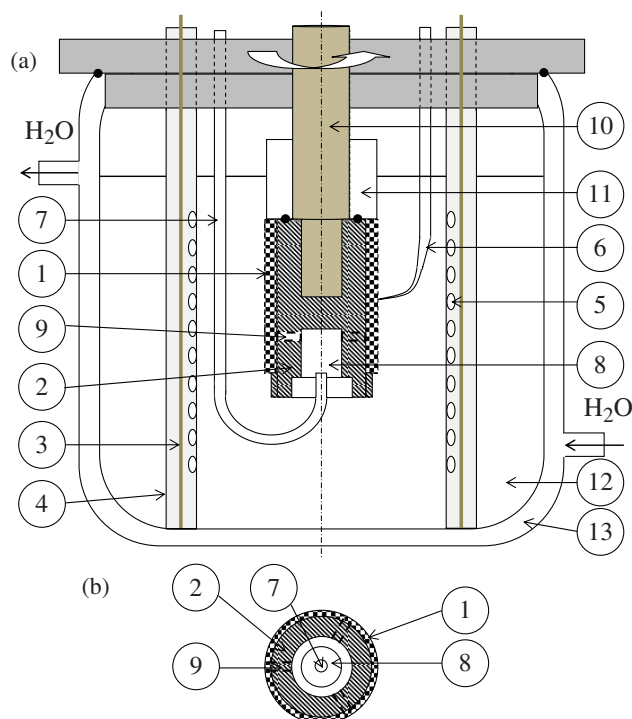

Figure 6. (a) Schematic view of the electrochemical reactor and (b) bottom view of the working electrode: 1, three-dimensional structure; 2, graphite support; 3, counter electrode; 4, anodic compartment; 5, window for the cationic exchange membrane; 6, Luggin capillary; 7, oxygen feeder; 8, oxygen chamber; 9, channels for oxygen distribution; 10, electrode shaft; 11, Teflon cylinder; 12, electrolyte container; 13, heating jacket.

is fed in the same place where it is consumed allowing the oxygen concentration to be maintained at its maximum value; and (ii) the structure of the three-dimensional cathode is also used as a gas distributor. The oxygen volumetric flow rate was 9.36×10^{-6} m^3 s^{-1}, under ambient conditions, and it was also bubbled through the solution for 1 h before the experiment to ensure that the electrolyte was saturated with oxygen.

Three nickel wires, 1.5 mm diameter and 120 mm long, were used as anodes. Each anode was separated from the cathodic compartment by a cationic exchange membrane inserted between two perforated Teflon tubes, giving three anodic compartments, 13.5 mm external diameter, placed symmetrically around the rotating electrode. The gap between the external surface of the RVC working electrode and the cationic exchange membrane was 12 mm. The working electrode and the counter electrode were concentric. Then, taking into account that the reaction is under mass-transfer control a uniform tertiary current distribution can be assumed. A saturated calomel electrode connected to a Luggin capillary located in the middle region at the external surface of the working electrode was used as a reference. In the cathodic compartment 0.5 mol L^{-1} NaOH was used as the electrolyte and 2 mol L^{-1} NaOH was used in the anodic compartments, which were frequently replenished with fresh solution to maintain the concentration and to avoid accumulation of the oxygen evolved at the anode. No chelating or other peroxide stabilizing agents were added to the catholyte. The electrolyte volume in the cathodic compartment was 0.6 L and approximately 20 cm^3 in the anodic part.

The experiments were performed galvanostatically at 30°C and changing the rotation speed. The cell voltage and the cathodic

potential against the saturated calomel electrode were measured. At the end of the experiment a sample of the solution was taken from the cathodic compartment and the hydrogen peroxide concentration was determined by titrating the acidified solution with potassium permanganate.[45]

Radial flow of the liquid and gas phases was established by rotation of the electrode. The oxygen volumetric flow rate was controlled with a gas pressure regulator. However, the liquid volumetric flow rate depends on the pressure difference between the inner and outer electrode surfaces produced by the centrifugal force and for a cylindrical configuration is given by:[46]

$$\Delta P = \left(r_o^2 - r_i^2 \right) \frac{\rho \omega^2}{2} \tag{8}$$

which must be counteracted by the pressure drop in the three-dimensional structure according to the Ergun equation:[47]

$$\frac{dP}{dr} = -\frac{A_s}{6\epsilon^3} \left(1.75 + \frac{25 A_s \nu}{u} \right) \rho u^2 \tag{9}$$

Integrating Equation (9) and combining with Equation (8) gives:

$$\frac{A_s}{3\epsilon^3} \left[\frac{0.4375 q^2}{(\pi L)^2} \left(\frac{1}{r_i} - \frac{1}{r_o} \right) + \frac{12.5 A_s \nu q}{\pi L} \ln \frac{r_o}{r_i} \right] = \left(r_o^2 - r_i^2 \right) \omega^2 \tag{10}$$

This equation with the above geometric parameters gives at 1000 rpm a liquid volumetric flow rate of approximately 1×10^{-3} m^3 s^{-1}, which is higher than the gas volumetric flow rate delivered by the pressure regulator. Then, it is expected that the hydrodynamic behaviour of the reactor, the mass transfer and the ohmic drop in the solution phase will be hardly influenced by the gas phase. Likewise, the high values of liquid volumetric flow rate associated with the turbulence promoting action of the reticulated structure produces good mass transfer conditions for the reduction of dissolved oxygen, which is continuously replenished by the co-current gas flow.

Results and discussion

The experiments with the rotating disc electrode together with the above analysis of the literature have shown that it is not possible to identify a range of potential where the oxygen reduction to hydrogen peroxide takes place as the only reaction. Thus, it is necessary to perform experiments with a laboratory reactor at different total currents in order to obtain the optimal value, which gives a maximum in the current efficiency for the production of hydrogen peroxide. Figure 7 shows the current efficiency as a function of the macrokinetic current density, defined as the ratio between the current and the external surface area of the three-dimensional electrode. All the experiments were galvanostatically performed until a charge of 1 A h was passed. It can be seen that the best performance is given by RVC 100, which shows the highest values of current efficiency. Figure 8 shows the specific energy consumption under the conditions given in Fig. 7. The minimum is obtained when three-dimensional structures of high specific surface area, such as RVC 45 and RVC 100, are used, and as expected E_s increases with increase in the macrokinetic current density. From Figs 7 and 8 it is concluded that using RVC100 at approximately 40 mA cm^{-2}, or a volumetric current density of 52 mA cm^{-3}, represents an appropriate choice for
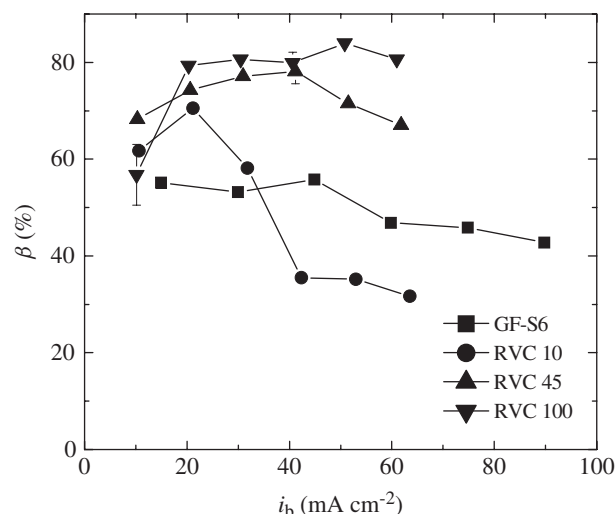
Figure 7. Current efficiency as a function of the macrokinetic current density. [NaOH] $= 0.5$ mol L^{-1}; $T = 30°$C; $P = 0.1$ MPa; $Q = 1$ A h; rotation speed: 1000 rpm. Vertical segments: standard error of the mean.
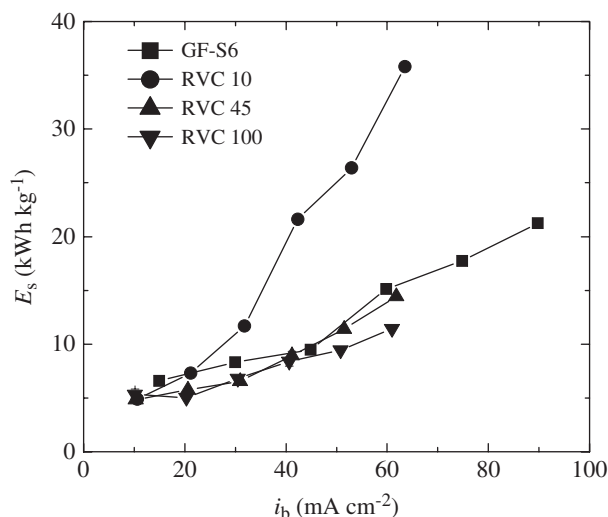
Figure 8. Specific energy consumption as a function of the macrokinetic current density. [NaOH] $= 0.5$ mol L^{-1}; $T = 30°$C; $P = 0.1$ MPa; $Q = 1$ A h; $\omega = 1000$ rpm. Vertical segments: standard error of the mean.

hydrogen peroxide production with a rotating three-dimensional cathode. An additional experiment performed under the above conditions but at 40°C yielded a current efficiency of only 71%, which corroborates that an increase in temperature favours the reduction and decomposition of hydrogen peroxide according to Equations (3) and (5), respectively.

Figure 9 shows the effect of rotation speed on the performance of the electrochemical reactor, where an important improvement of reactor performance was detected when the rotation speed was increased from 500 to 1000 rpm. However, with further increase of the rotation speed to 1500 rpm the important figures decrease, because of the formation of an electrolyte vortex in the three-dimensional structure which decreases the electrode surface area. No important differences in the behaviour of the reactor were observed when the oxygen volumetric flow rate was decreased to 3.04×10^{-6} m^3 s^{-1}, confirming the presence of excess oxygen
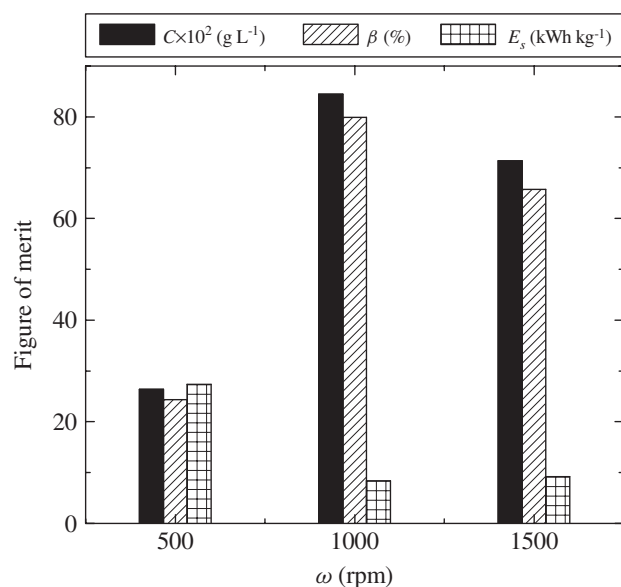
Figure 9. Figures of merit as a function of the rotation speed. [NaOH] = 0.5 mol L^{-1}; T = 30°C; P = 0.1 MPa; I = 2 A; t = 30 min; i_b = 40 mA cm^{-2}. RVC 100 ppi.

Figure 10. Hydrogen peroxide concentration as a function of electrolysis time. [NaOH] = 0.5 mol L^{-1}; T = 30°C; P = 0.1 MPa; ω = 1000 rpm; I = 2 A; i_b = 40 mA cm^{-2}. RVC 100 ppi.

Figure 11. Current efficiency (●) and specific energy consumption (▲) as a function of electrolysis time. [NaOH] = 0.5 mol L^{-1}; T = 30°C; P = 0.1 MPa; ω = 1000 rpm; I = 2 A; i_b = 40 mA cm^{-2}. Vertical segments: standard error of the mean. RVC 100 ppi.

and that the gas phase has no influence on the hydrodynamic conditions inside the electrode.

The hydrogen peroxide concentration, current efficiency and specific energy consumption are shown in Figs 10 and 11 for experiments performed for different times of electrolysis using RVC 100 as a three-dimensional electrode with a total current of 2 A, which gave a theoretical fractional conversion of 2.75% for oxygen to hydrogen peroxide. Therefore, the oxygen feed is in excess of the stoichiometric quantity. In these figures each point corresponds to an independent experiment. As expected for galvanostatic experiments in a batch reactor, a linear increase of the concentration is detected with approximately constant values of the other figures of merit when the duration of the experiment was lower than 6 h. The concentration of hydrogen peroxide under these conditions of 6 h electrolysis, i_b = 40 mA cm^{-2}, rotation speed = 1000 rpm, T = 30°C was 8.4 g L^{-1}, that is a current efficiency of 80.5% and specific energy consumption 8.41 kWh kg^{-1}. However, for long-term experiments the hydrogen peroxide concentration approaches a maximum value of approximately 10.4 g L^{-1} with a decrease in current efficiency and increase in the specific energy consumption, which can be explained due to hydrogen peroxide destruction according to Equations (3) and (5). The final concentration of sodium hydroxide after 8 and 10 h electrolysis was 1.33 and 1.41 mol L^{-1}, respectively. The cathodic potential against a saturated calomel electrode ranged from −1.2 to −1.4 V and the cell voltage from 3.9 to 4.6 V with a mean value of 4.2 V. The electrochemical and rotational power requirements were 8.4 and 2.3 W, respectively. In all these experiments it was observed that the electrolyte volume of the cathodic compartment increases due to the inlet of the water of hydration of sodium ions, which migrate through the membrane from the anodic compartment. The above results show a lower performance than reported for the previous processes,[4] which demands further efforts in the development of an alternative reactor based on the present proposal. However, similar results were reported by Gyence and Oloman[48] using a small-scale batch electrochemical reactor with reticulated vitreous carbon of 30 ppi and using 0.1 mol L^{-1} Na$_2$CO$_3$
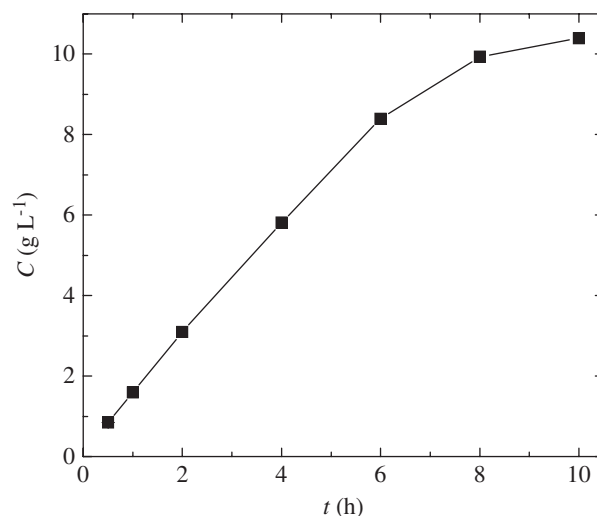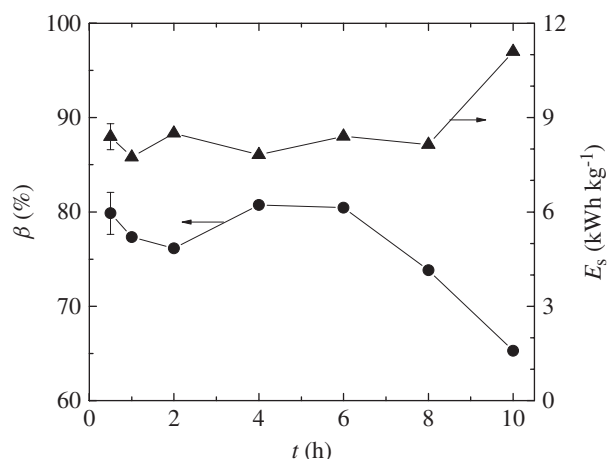
as electrolyte with a surfactant, where the hydrogen peroxide concentration and current efficiency increased with surfactant concentration.

CONCLUSIONS

1 Results from the rotating disc electrode showed that 0.5 mol L^{-1} NaOH for the concentration of supporting electrolyte and 30°C temperature were appropriate operating conditions for hydrogen peroxide production. However, from the polarization curves it was not possible to identify a potential range where the only reaction was oxygen reduction to hydrogen peroxide.

2 Experiments with rotating cylinder electrodes showed that the best performance was given by a reticulated vitreous carbon 100 ppi at 30°C, 1000 rpm and 40 mA cm^{-2}. Constant values of current efficiency and specific energy consumption were obtained up to 6 h of electrolysis. Further increases in the

temperature and in the macrokinetic current density decreased the reactor performance.

3 The concept, operating mode and application to the production of hydrogen peroxide of a three-dimensional rotating cylinder electrode with a co-current flow of the gas and liquid phases in radial direction were described. The experimental results showed that this reactor may become an attractive device for the synthesis of hydrogen peroxide from initially dilute alkaline solutions. Further research and development efforts are necessary to obtain an alternative reactor either for this application, showing similar performance to previous processes, or in general, for carrying out electrochemical reactions with gaseous reactants.

REFERENCES

1 Kirk RE and Othmer DF, *Encyclopedia of Chemical Technology*, 4th edn. Wiley - Interscience, New York, Volume 13, 470 (1993).

2 Goor G, Glenneberg J and Jacobi S, Hydrogen peroxide, in *Ullmann's Encyclopedia of Industrial Chemistry*. Wiley-VCH Verlag GmbH & Co. KGaA, Weinheim, (2007).

3 Berl E, A new cathodic process for the production of H_2O_2, *Trans Electrochem Soc* **76**:359–369 (1939).

4 Foller PC and Bombard RT, Processes for the production of mixtures of caustic soda and hydrogen peroxide via the reduction of oxygen, *J Appl Electrochem* **25**:613–627 (1995).

5 Oloman C, *Electrochemical Processing for the Pulp and Paper Industry*. The Electrochemical Consultancy Ltd., Romsey Hants, England, 143–152 (1996).

6 Oloman C and Watkinson P, The electroreduction of oxygen to hydrogen peroxide on fluidized cathodes. *Can J Chem Eng* **53**:268–273 (1973).

7 Alvarez-Gallegos A and Pletcher D, The removal of low level organics via hydrogen peroxide formed in a reticulated vitreous carbon cathode cell, Part 1. The electrosynthesis of hydrogen peroxide in aqueous acidic solutions. *Electrochim Acta* **44**:853–861 (1998).

8 Alvarez-Gallegos A and Pletcher D, The removal of low level organics via hydrogen peroxide formed in a reticulated vitreous carbon cathode cell. Part 2. The removal of phenols and related compounds from aqueous effluents. *Electrochim Acta* **44**:2483–2492 (1999).

9 Oloman C, Trickle bed electrochemical reactors. *J Electrochem Soc* **126**:1885–1892 (1979).

10 Špalek O and Balogh K, Reduction of oxygen to peroxide in a trickle electrode. *Collect Czech Chem Commun* **54**:1564–1574 (1989).

11 Špalek O and Balogh K, Generation of hydrogen peroxide by reduction of oxygen in semihydrophobic trickle electrodes. *Collect Czech Chem Commun* **56**:309–316 (1991).

12 Yamada N, Yaguchi T, Otsuka H and Sudoh M, Development of trickle-bed electrolyzer for on-site electrochemical production of hydrogen peroxide. *J Electrochem Soc* **146**:2587–2591 (1999).

13 Yamada N, Yaguchi T and Sudoh M, Oxygen-utilization performance of trickle-bed cathode for on-site electrochemical production of hydrogen peroxide. *Electrochemistry* **69**:154–159 (2001).

14 Gupta N and Oloman C, Scale-up of the perforated bipole trickle-bed electrochemical reactor for the generation of alkaline peroxide. *J Appl Electrochem* **36**:1133–1141 (2006).

15 Gupta N and Oloman C, Modeling a perforated bipole trickle bed electrochemical reactor for the generation of alkaline peroxide. *J Appl Electrochem* **38**:131–149 (2008).

16 Haggin J, Trickle-bed electrolytic cell for peroxide developed. *Chem Eng News* **12**:16 (1984).

17 Špalek O, Balej J and Balogh K, Preparation of hydrogen peroxide by cathodic reduction of oxygen in porous electrodes made of different carbonaceous materials. *Collect Czech Chem Commun* **42**:952–959 (1977).

18 Reis RM, Beati AAGF, Rocha RS, Assumpção MHMT, Santos MC, Bertazzoli R and Lanza MRV, Use of gas diffusion electrode for the *in situ* generation of hydrogen peroxide in an electrochemical flow-by reactor. *Ind Eng Chem Res* **51**:649–654 (2012).

19 Brezina M and Hofmanová A, Study of the electrochemical reduction of oxygen on glassy carbon in an alkaline medium. *Collect Czech Chem Commun* **38**:985–993 (1973).

20 Davison JB, Kacsir JM, Peerce-Landers PJ and Jasinski R, A voltammetric investigation of oxygen reduction in a trickle bed cell using graphite chip and RVC cathodes. *J Electrochem Soc* **130**:1497–1501 (1983).

21 Ponce De Leon C and Pletcher D, Removal of formaldehyde from aqueous solutions via oxygen reduction using a reticulated vitreous carbon cathode cell. *J Appl Electrochem* **25**:307–314 (1995).

22 Xu J, Huang W and McCreery RL, Isotope and surface preparation effects on alkaline dioxygen reduction at carbon electrodes. *J Electroanal Chem* **410**:235–242 (1996).

23 Ragnini CAR, Di Iglia RA and Bertazzoli R, Considerações sobre a electrogeração de peróxido de hidrogênio. *Quim Nova* **24**:252–256 (2001).

24 Wang F and Hu S, Studies of electrochemical reduction of dioxygen with RRDE. *Electrochim Acta* **51**:4228–4235 (2006).

25 Knoll J and Swavey S, Electrocatalytic reduction of protons and oxygen at glassy carbon electrodes coated with a cobalt(II)/platinum(II) porphyrin. *Inorg Chim Acta* **362**:2989–2993 (2009).

26 Bonakdarpour A, Esau D, Cheng H, Wang A, Gyenge E and Wilkinson DP, Preparation and electrochemical studies of metal–carbon composite catalysts for small-scale electrosynthesis of H_2O_2. *Electrochim Acta* **56**:9074–9081 (2011).

27 Wu J, Zhang D, Wang Y, Wan Y and Hou B, Catalytic activity of graphene–cobalt hydroxide composite for oxygen reduction reaction in alkaline media. *J Power Sources* **198**:122–126 (2012).

28 Gorlin Y, Chung C-J, Nordlund D, Clemens BM and Jaramillo TF, Mn_3O_4 supported on glassy carbon: an active non-precious metal catalyst for the oxygen reduction reaction, *ACS Catal* **2**:2687–2694 (2012).

29 Mo G, Liao S, Zhang Y, Zhang W and Ye J, Synthesis of active iron-based electrocatalyst for the oxygen reduction reaction and its unique electrochemical response in alkaline medium. *Electrochim Acta* **76**:430–439 (2012).

30 Taylor RJ and Humffray AA, Electrochemical studies on glassy carbon electrodes: II. Oxygen reduction in solutions of high pH (pH > 10). *J Electroanal Chem* **64**:63–84 (1975).

31 Baez VB and Pletcher D, Preparation and characterization of carbon/titanium dioxide surfaces - the reduction of oxygen. *J Electroanal Chem* **382**:59–64 (1995).

32 Tammeveski K, Kontturi K, Nichols RJ, Potter RJ and Schiffrin DJ, Surface redox catalysis for O_2 reduction on quinone-modified glassy carbon electrodes. *J Electroanal Chem* **515**:101–112 (2001).

33 Sarapuu A, Vaik K, Schiffrin DJ and Tammeveski K, Electrochemical reduction of oxygen on anthraquinone-modified glassy carbon electrodes in alkaline solution. *J Electroanal Chem* **541**:23–29 (2003).

34 Vaik K, Sarapuu A, Tammeveski K, Mirkhalaf F and Schiffrin DJ, Oxygen reduction on phenanthrenequinone-modified glassy carbon electrodes in 0.1 M KOH. *J Electroanal Chem* **564**:159–166 (2004).

35 Vaik K, Mäeorg U, Maschion FC, Maia G, Schiffrin DJ and Tammeveski K, Electrocatalytic oxygen reduction on glassy carbon grafted with anthraquinone by anodic oxidation of a carboxylate substituent. *Electrochim Acta* **50**:5126–5131 (2005).

36 Jürmann G, Schiffrin DJ and Tammeveski K, The pH-dependence of oxygen reduction on quinone-modified glassy carbon electrodes. *Electrochim Acta* **53**:390–399 (2007).

37 Maia G, Maschion FC, Tanimoto ST, Vaik K, Mäeorg U and Tammeveski K, Attachment of anthraquinone derivatives to glassy carbon and the electrocatalytic behavior of the modified electrodes toward oxygen reduction. *J Solid State Electrochem* **11**:1411–1420 (2007).

38 Isaacs M, Aguirre MJ, Toro-Labbé A, Costamagna J, Paéz M and Zagal JH, Comparative study of the electrocatalytic activity of cobalt phthalocyanine and cobalt naphthalocyanine for the reduction of oxygen and the oxidation of hydrazine. *Electrochim Acta* **43**:1821–1827 (1998).

39 Kullapere M, Jürmann G, Tenno TT, Paprotny JJ, Mirkhalaf F and Tammeveski K, Oxygen electroreduction on chemically modified glassy carbon electrodes in alkaline solution. *J Electroanal Chem* **599**:183–193 (2007).

40 Geng D, Liu H, Chen Y, Li R, Sun X, Ye S and Knights S, Non-noble metal oxygen reduction electrocatalysts based on carbon nanotubes with controlled nitrogen contents. *J Power Sources* **196**:1795–1801 (2011).

41 Bard AJ and Faulkner LR, *Electrochemical Methods: Fundamental and Applications*, 2nd edn. John Wiley & Sons, New York, 341 (2001).

42 Kinoshita K, *Electrochemical Oxygen Technology*. John Wiley & Sons, New York, 9–10 (1992).

43 Kreysa G, Jüttner K and Bisang JM, Cylindrical three-dimensional electrodes under limiting current conditions. *J Appl Electrochem* **23**:707–714 (1993).

44 Nahlé AH, Reade GW and Walsh FC, Mass transport to reticulated vitreous carbon rotating cylinder electrodes. *J Appl Electrochem* **25**:450–455 (1995).

45 Vogel AI, *Vogel's Textbook of Quantitative Chemical Analysis*, 5th edn. Longman, Essex, 372–373 (1989).

46 McCabe WL, Smith JL and Harriott P, *Unit Operations of Chemical Engineering*, 7th edn. McGraw-Hill, New York, 1031 (2005).

47 Bird RB, Stewart WE and Lightfoot EN, *Transport Phenomena*, 2nd edn. John Wiley & Sons, New York, 191 (2002).

48 Gyenge EL and Oloman CW, Influence of surfactants on the electroreduction of oxygen to hydrogen peroxide in acid and alkaline electrolytes. *J Appl Electrochem* **31**:233–243 (2001).

535